Reprint from

"ATOMIC ENERGY REVIEW"
Vol.12, No.4

INTERNATIONAL ATOMIC ENERGY AGENCY
VIENNA, 1974

THE USE OF ENDOR IN SOLID-STATE SPECTROSCOPY

C.A.J. AMMERLAAN
Natuurkundig Laboratorium,
University of Amsterdam,
Amsterdam,
The Netherlands

ABSTRACT. The application of electron nuclear double resonance (ENDOR) in research into the inorganic solid state is reviewed. In an introduction the transient, stationary, and distant ENDOR mechanisms are discussed, followed by some considerations on the sensitivity and resolution of the technique. A separate section gives some details of experimental procedures and the design of ENDOR cavities. Then the field of applications of ENDOR — defects in alkali halides and in semiconductors, and paramagnetic impurities in diamagnetic lattices — is briefly described. Two examples are treated in more detail, manganese-doped fluorides and shallow and deep-level impurities in silicon.

1. INTRODUCTION

Figure 1 shows the number of ENDOR papers published each year since Feher's invention of this method in 1956 [1-3]. The steady increase reflects the growing appreciation of solid-state physicists for this powerful spectroscopical technique.

2. PRINCIPLES OF ENDOR

2.1. Energy levels

The word ENDOR is an acronym formed from Electron Nuclear DOuble Resonance. In this double magnetic resonance method aspects of electron paramagnetic resonance (EPR) and nuclear magnetic resonance (NMR) are combined. The method is applicable in systems in which an interaction exists between electronic and nuclear magnetic moments. To illustrate the basic ideas of ENDOR, consider a system with both the electron and nuclear spin equal to 1/2: $S = 1/2$, $I = 1/2$ (for example P in Si). The spin Hamiltonian for this simple case reads:

$$\mathscr{H} = g_e\mu_B\vec{H}\cdot\vec{S} - g_N\mu_N\vec{H}\cdot\vec{I} + A\vec{S}\cdot\vec{I}$$

Again for the sake of simplicity we take scalar quantities for the electronic g-factor g_e and for the hyperfine interaction constant A. In the limit of

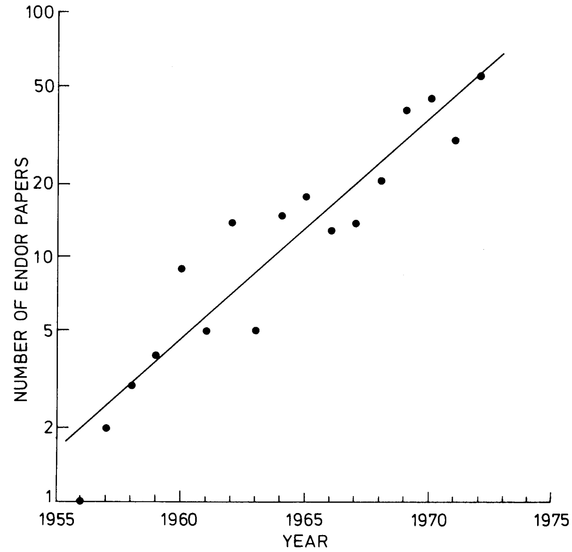

FIG. 1. Number of ENDOR papers by year, reporting research in the inorganic solid state.

high magnetic field $\vec{H}$ the solutions of the eigenvalue equation are the four eigenstates $|m_S, m_I\rangle$, with $m_S = \pm 1/2$, $m_I = \pm 1/2$. The four corresponding energy eigenvalues, as shown in Fig. 2, are given by:

$$E = g_e\mu_B Hm_S - g_N\mu_N Hm_I + Am_S m_I$$

In Fig. 2(a) the allowed transitions between the levels are indicated. EPR transitions, which have their frequency in the microwave region, require a change of the electron spin quantum number by one: $\Delta m_S = \pm 1$, $\Delta m_I = 0$. For NMR transitions, occurring at radiofrequencies, the nuclear spin quantum number changes by one: $\Delta m_I = \pm 1$, $\Delta m_S = 0$. In thermal equilibrium, Fig. 2(a), the levels are occupied according to the Boltzmann distribution law. Since the nuclear Boltzmann factor $g_N\mu_N H/kT$ is roughly 1000 times smaller than the electronic Boltzmann factor $g_e\mu_B H/kT \equiv 2\epsilon$ ($\mu_B/\mu_N = 1836$), the effect of the former is neglected in calculating level populations.

2.2. Transient ENDOR

For the application of transient ENDOR the values of magnetic field and microwave frequency are adjusted to obey one of the two electron resonance conditions. This is indicated for ν_{e1} in Fig. 2(b). The microwave power is chosen so high that the transition is saturated. In the extreme case, as in Fig. 2(b), full saturation is achieved, the populations of the two levels involved are equalized and the EPR signal will be small. Under these saturation conditions an NMR transition is induced, e.g. the transition $h\nu_{N1}$ connecting the highest two states. The NMR transition will lower the population of the $|+1/2, +1/2\rangle$-level, resulting in a transient increase of

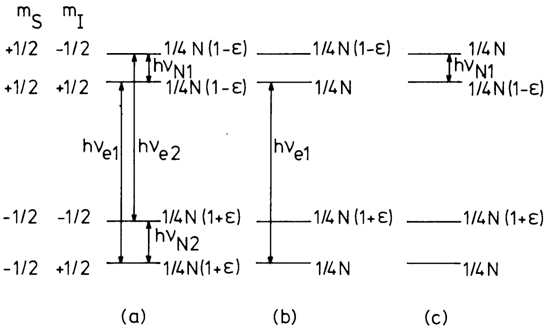

FIG. 2. Energy levels of the spin system $S = 1/2$, $I = 1/2$ in an externally applied large magnetic field, and level populations under various conditions: (a) populations in thermal equilibrium; (b) after saturating the EPR transition $h\nu_{e1}$; (c) after adiabatic fast passage through the nuclear transition $h\nu_{N1}$.

the EPR amplitude. This is a characteristic aspect of the ENDOR method: the induction of nuclear magnetic resonance is observed by a change of the electron spin resonance intensity. The induction of the nuclear transition may either be a saturation at high RF power equalizing the level populations, or an adiabatic fast passage in which the populations of the levels are reversed. This latter case is illustrated in Fig. 2(c). ENDOR based on this mechanism only produces a transient signal. Before observing the ENDOR signal a second time one must go off resonance and allow the spin system sufficient time to relax to the situation as sketched in Fig. 2(b). Feher's first ENDOR experiments, carried out on phosphorus doped silicon [3-5] and on the F centre in KCl [6], are examples of the transient ENDOR technique. These experiments are performed at low temperatures where relaxation times are very long. One of the results is shown in Fig. 3.

2.3. Stationary ENDOR

As for the previous method, a necessary requirement is again that one of the EPR lines is saturated. The amplitude of the EPR line will then be dependent upon the spin-lattice relaxation time τ_{SL} [7-10]. It now turns out to be possible to change effectively this relaxation time in an ENDOR experiment. For an explanation of the mechanism, consider Fig. 4. In the normal situation, without RF, the electron spins can only relax via the usual spin-lattice relaxation process, a path indicated by τ_{SL} in Fig. 4. However, if the two nuclear levels are short-circuited by applying RF at saturation power, a second relaxation path, involving the cross-relaxation τ_X, acts in parallel with the normal spin-lattice relaxation [11, 12]. This results in a slightly lower effective relaxation time τ'_{SL}, expressed by the relation: $(\tau'_{SL})^{-1} = \tau_{SL}^{-1} + \tau_X^{-1}$. Since the EPR amplitude depends in magnitude on the actual relaxation time, the change in τ_{SL} brings about a steady change of EPR amplitude. This is the stationary ENDOR signal.

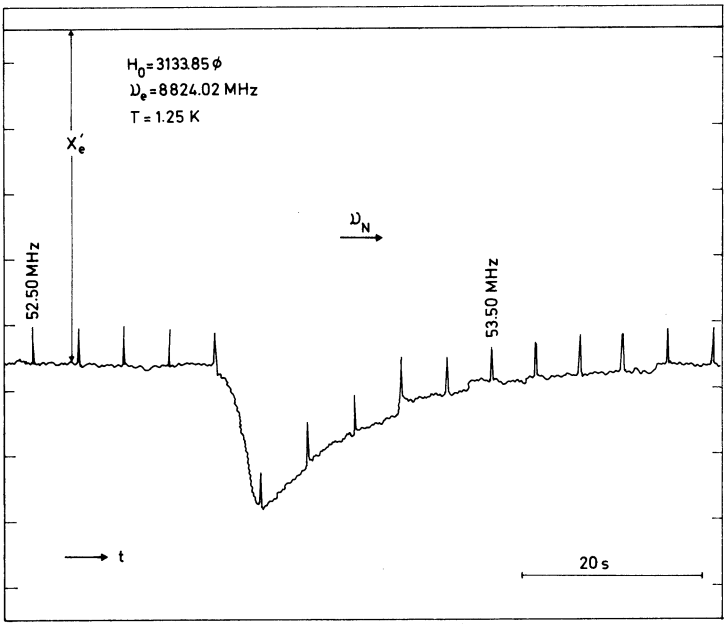

FIG. 3. A typical result of a transient ENDOR experiment performed by Feher on phosphorus doped silicon [3].

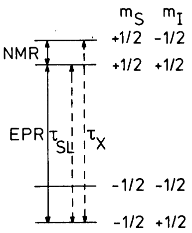

FIG. 4. Illustration of the stationary ENDOR mechanism. Full arrows indicate the transitions induced by EPR and NMR. Spin-lattice relaxation and cross relaxation paths are labelled with τ_{SL} and τ_X, respectively.

Electron-nuclear cross-relaxation itself is a consequence of the hyperfine interaction. This may be seen by writing down the hyperfine term of the spin Hamiltonian:

$$A\vec{S}\cdot\vec{I} = AS_zI_z + \tfrac{1}{2}A(S_+I_- + S_-I_+)$$

The hyperfine interaction contains terms that increase the electron spin quantum number by one, while simultaneously lowering the nuclear spin quantum number by one, and vice versa. If phonons of the required frequency are present, cross-relaxation processes will be induced. Hale and Mieher [13] have investigated the shallow donors in silicon by ENDOR under conditions in which the stationary mechanism prevails. One of their results is reproduced as Fig. 5.

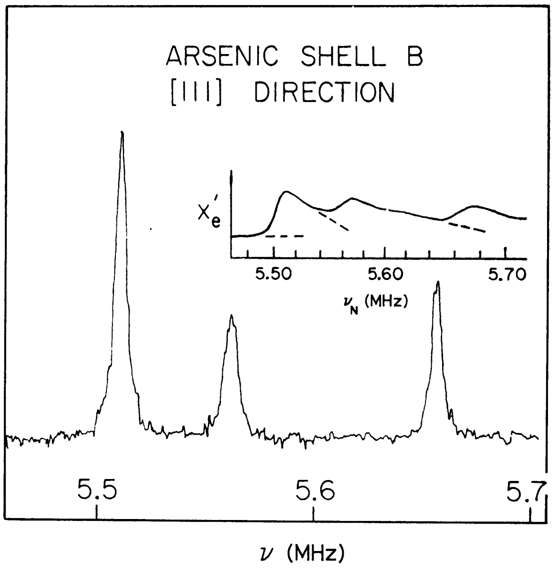

FIG. 5. ENDOR spectra in arsenic doped silicon with $\vec{H}$ along a [111] crystal direction. The upper trace is taken from Feher's work by the stationary ENDOR method [5]; the lower trace from Hale and Mieher's experiments with stationary ENDOR [13].

2.4. Distant ENDOR

A completely different ENDOR mechanism was proposed by Lambe et al. [14] as a result of their investigations of double resonance in ruby crystals (Al_2O_3 containing Cr^{3+}-ions). They observed ENDOR at the aluminium nuclear resonance frequency, without the shifts due to addition or subtraction of hyperfine interactions. They therefore established ENDOR effects, even when spins of aluminium nuclei were flipped far apart from the Cr^{3+}-ions of which an EPR transition was being monitored. Since remote nuclei are responsible for this ENDOR, the phrase distant ENDOR, in contrast to the local ENDOR of the previous section, was coined for this phenomenon. The interaction between the spins presumably occurs by spin diffusion and has a characteristic time comparable to nuclear, rather than electronic, relaxation times. In more dilute ruby (0.01% Cr) the distant ENDOR signals were of relatively less importance. It proved to be necessary to distinguish clearly between ENDOR effects on the dispersive and absorptive parts of the electronic susceptibility. While there is an asymmetric skewing of the dispersion curve, the effect on the absorption is a more uniform and moderate increase.

2.5. Sensitivity

The net number of transitions induced when applying radiation of the resonant frequency is proportional to the difference in population of the two levels involved. In a regular NMR experiment this difference is governed by the nuclear Boltzmann factor. However, in an ENDOR experiment, through the pumping action of the microwave quanta, this difference is greatly enhanced. Two levels, as in Fig.2(b), which are connected by the RF-field, now have a population difference that is characterized by the much larger electron Boltzmann factor. This represents a considerable increase in sensitivity when detecting an NMR transition by means of the ENDOR technique over the direct detection method. Moreover, the level populations become independent of the nuclear magnetic moment so that nuclei with small moments do not suffer from the usual loss in sensitivity.

2.6. Resolution

From the solution of the eigenvalue equation, section 2.1, it is seen that EPR transitions will be found for

$$h\nu_{e1,2} = g_e \mu_B H \pm \tfrac{1}{2} A$$

If there is only one nuclear magnetic moment with which the electron interacts, i.e. one A, which is not too small, the spectrum will already be resolved completely in EPR. Usually, however, there is a whole variety of N nuclei at different positions in the lattice with respect to the paramagnetic centre, each having their own hyperfine interaction constant. In consequence, a summation must be made over all these nuclei and the formula must be modified to:

$$h\nu_e = g_e \mu_B H + \sum_{j=1}^{N} A_j m_{Ij} \qquad m_{Ij} = \pm 1/2 \quad j = 1, \ldots\ldots, N$$

In many cases the separation between the 2^N various possible transition frequencies is less than the homogeneous linewidth of the individual spin packets. In such a case the EPR line cannot be resolved into its constituting components, but instead the envelope of it will be measured. The line is said to be inhomogeneously broadened.

For the NMR transitions of the kth nucleus the frequencies will be given by

$$h\nu_{Nk} = g_N \mu_N H \pm \tfrac{1}{2} A_k \qquad k = 1, \ldots\ldots, N$$

The width of these lines is the homogeneous linewidth of the nuclear transitions, to which a possible unresolved inhomogeneous broadening due to interactions between the nuclei has to be added. In many practical cases, e.g. the colour centres in alkali halides, the NMR linewidth is 3 to 4 orders of magnitude smaller than that observed in EPR. This represents an enormous gain in resolving power. This fact, together with the increased sensitivity as discussed under section 2.5, is at the basis of the successful application of ENDOR spectroscopy in solid-state research.

3. EQUIPMENT FOR ENDOR

To carry out an ENDOR experiment it is necessary to add to an EPR spectrometer the facility of inducing nuclear transitions. Since in ENDOR

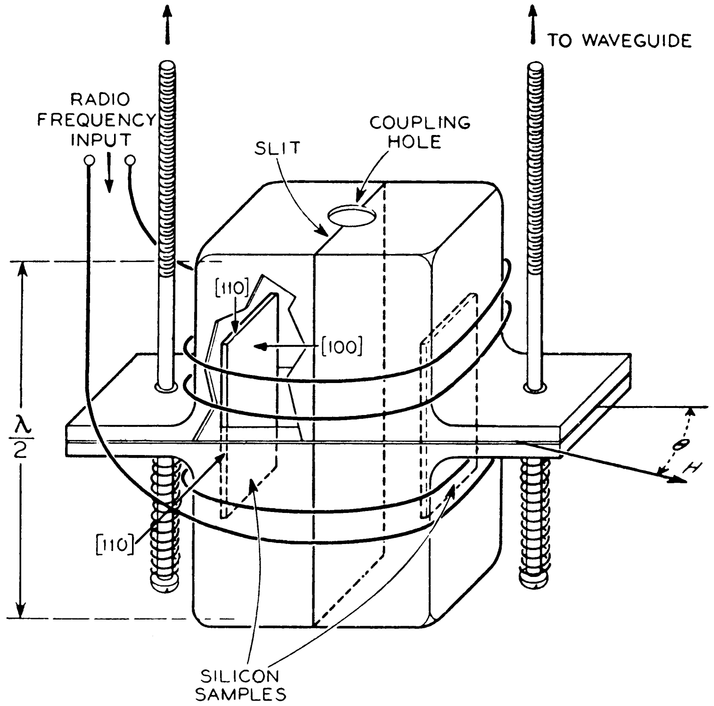

FIG. 6. The ENDOR cavity of Feher [5].

the signal to be detected is a change of an EPR amplitude, no specific RF detection unit, as in an NMR spectrometer, is required. The radiofrequencies to be applied to the sample usually fall in the range from 1 to 1000 MHz. In a normal set-up this frequency is slowly scanned by changing, with the help of a motor drive, the output frequency of an RF oscillator. The RF signal may be amplified, using a wide-band amplifier, to attain RF fields H_2 in the cavity up to about 1 Oe. In most ENDOR experiments the RF current is sinusoidally or square-wave on-off amplitude modulated at an audio-frequency, with no modulation of the magnetic field. Phase-sensitive detection with the applied RF is then employed. Occasionally a double-modulation technique of both RF and magnetic field has been used [13]. This offers some advantages, certainly in the case of weak and narrow EPR signals.

The most characteristic change required by ENDOR is the modification of the microwave cavity to allow for the introduction of the radiofrequency field. A number of solutions to this problem have been described in the literature. Feher [5] originally wrapped a coil on the outside of his TE_{101} cavity, while slits in the walls allow the nuclear frequency to penetrate the cavity (Fig. 6). In their investigations of ruby Lambe et al. [14] put the RF coil, consisting of two turns of fine copper wire, inside the cavity (Fig. 7). A similar arrangement for a TE_{102} cavity was adopted by Schrama [15], who preferred a single loop coil of 1 mm copper wire strongly clamped

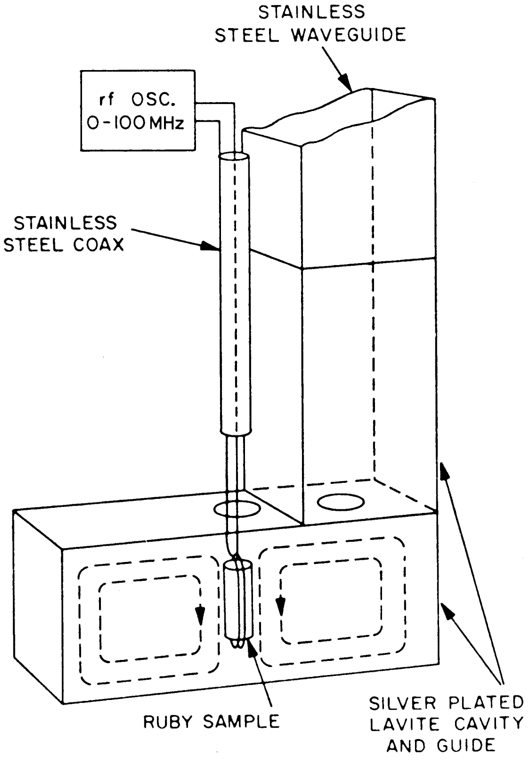

FIG. 7. The ENDOR cavity of Lambe et al. [14].

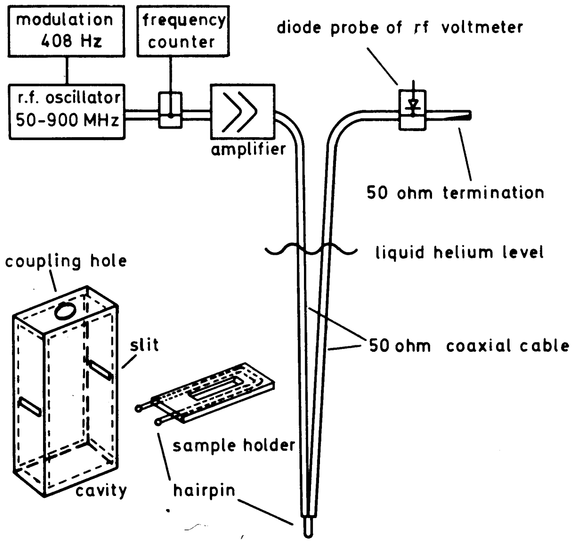

FIG. 8. The ENDOR cavity of Schrama [15].

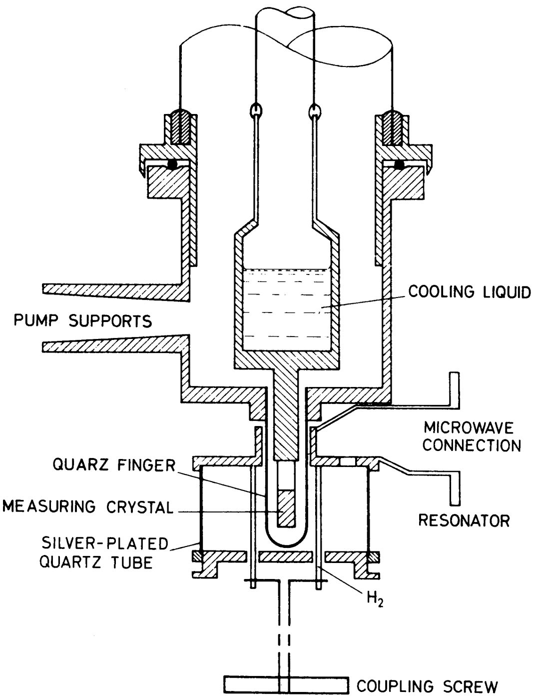

FIG. 9. The ENDOR cavity of Seidel [16].

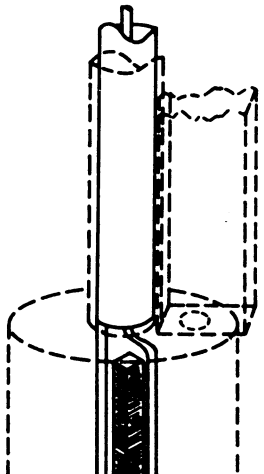

FIG. 10. The ENDOR cavity of Watkins and Corbett [17].

in the cavity walls (Fig. 8). Figure 9 shows the cylindrical ENDOR cavity used by Seidel [16]. The two loops of the coil are positioned in a Helmholtz configuration in order to improve the H_2 homogeneity over the sample volume. Finally Fig. 10 pictures the single-turn coil assembly of Watkins and Corbett [17], which can be inserted in and removed from the TE_{011} cylindrical cavity without disassembling the whole cryostat. In all these constructions the copper wires run perpendicular to the electric field lines of the standing wave pattern in the excited cavity. This is a necessary requirement to avoid ohmic losses through conduction in the wires, with their inherent degradation of the cavity quality factor. In a design by Woodbury and Ludwig [18] the side walls of a cylindrical cavity were given the form of a helix. This side wall serves the dual purpose of being microwave cavity wall and RF coil at the same time. A pretty drawing of this cavity is given in the book of Alger [19], who also discusses the merits of this and some other cavity configurations. Many more double-resonance cavities have been described in the literature [20-28].

4. APPLICATIONS OF ENDOR

As explained in the discussion of the principles of ENDOR, this technique is applicable to systems in which the nuclei are coupled to magnetic moments due to unpaired electron spins. These interactions are frequently small and lead to unresolved inhomogeneous broadening in EPR. ENDOR is often able to resolve the splittings to a large degree. A number of suitable systems exists.

4.1. Defects in alkali halides

No doubt the subject of colour centres in alkali halides represents the branch of physics in which the most thorough study of a great variety of crystal lattice defects has been made. These investigations include a number of intrinsic point defects, of which the F centre, an anion-vacancy that has trapped one electron, is the most famous. However, centres have also been discovered that are aggregates of a few point defects or for which an impurity (hydrogen, nitrogen, oxygen) is an essential constituent. EPR and ENDOR have played a vital role in the identification of these defects, and in their detailed description. The subject is too large to be discussed here; instead reference is made to some recent reviews [29-32].

4.2. Transition metals

Transition metal ions exhibit paramagnetic moments arising from their unfilled 3d shell. When dissolved into a diamagnetic host lattice their interactions with neighbouring nuclei and also with the nucleus of the paramagnetic impurity itself can be investigated by ENDOR, often referred to respectively as ligand ENDOR and self ENDOR. This has been done in a great number of cases, including, for instance, V^{2+} [33], Cr^{3+} [34-36], Mn^{2+} [36-41], Fe^{3+} [36, 42], and Co^{2+} [43] in MgO. A similar extensive series of experiments exists for corundum (Al_2O_3) as the host crystal. One example will be treated in more detail in the next section.

4.3. Rare earth metals

This field is strongly related conceptually to that of the transition metals. It will not be discussed in this paper.

4.4. Imperfections in semiconductors

The first ENDOR experiment concerned an impurity in a semiconductor, namely phosphorus in silicon. Since then many more ENDOR experiments have been performed on impurities and intrinsic defects in semiconductors, mainly in silicon, but also a few in materials like SiC [44,45], CdS [46-48], and CdTe [49-51]. The work on silicon will be reviewed in section 6.

4.5. Free radicals in solution

Following Cederquist's first paper reporting an ENDOR experiment on a paramagnetic centre in a liquid solvent [52] the ENDOR technique has been used intensively to study hyperfine interactions in organic free radicals in solution. Among the radicals in which proton hyperfine interactions were observed are Coppinger's radical [53-55], phenoxy radicals [56], perynaphthenyl radical [57,58] and tri-t-butylphenoxyl radical [57, 59]. Nitrogen ENDOR has been observed recently in nitroxide radicals [60, 61]. Usually only the isotropic interactions, i.e. the traces of the hyperfine tensors, are determined. In isotropic solvents the anisotropic contributions are averaged out by the Brownian motion of the molecules. Only in favourable cases can the width of the hyperfine lines be used to extract information on the anisotropic interactions. By performing ENDOR at the turning points of the EPR spectrum a complete hyperfine tensor, including anisotropy, has been determined for the carbazyl radical [62]. Another method for determining anisotropic tensor components is the use of liquid crystals as a solvent. Alignment can be achieved by applying a magnetic field in the nematic mesophase [57]. From ENDOR experiments valuable information for structure determination is obtained.

Electron spin-lattice relaxation is rapid in these systems. To induce observable ENDOR transitions high values of the radiofrequency field, typically 50 G continuous wave in the rotating frame, are required.

4.6. Spin relaxation processes

As explained in the paragraph on the principles of ENDOR, electron and nuclear spin relaxation processes are essential in the ENDOR mechanism. So the angle of vision may be reversed and ENDOR may be applied in the study of relaxation mechanisms. Valuable information on the dynamics of spin relaxation is contained in the theoretical papers dealing with the physical principles underlying ENDOR [12, 63-65]. In other cases double resonance techniques have been utilized experimentally to obtain data on spin relaxation rates [66,67].

5. MANGANESE-DOPED FLUORIDES

A very complete series of ENDOR experiments was carried out by Schrama on the Mn^{2+} ion incorporated in the isomorphous compounds

K_2MgF_4, K_2ZnF_4, K_2CdF_4, and Rb_2MgF_4, Rb_2ZnF_4, Rb_2CdF_4 [15, 68-70]. According to Hund's rules, the manganese, which substitutes for Mg, Zn, or Cd in these crystals, assumes a $3d^5\ {}^6S_{5/2}$ orbital singlet ground state. The electronic spin therefore is $S = 5/2$. The nuclear spin of ^{55}Mn has the same value: $I = 5/2$. The ENDOR spectrum consists of 30 allowed transitions: six groups, corresponding to the six possible values of m_S, with five nuclear transitions each. Analysis of such spectra requires a much more complicated spin Hamiltonian than the one introduced in section 2. To start with, in these compounds with axial symmetry around the Mn-site the g-factor and hyperfine interaction constant become tensors with different principal values for the parallel and perpendicular directions: $g_{\parallel}$, $g_{\perp}$, A (for $\parallel$) and B (for $\perp$). The spin Hamiltonian has further to be augmented by terms that account for crystal field splittings, the nuclear quadrupole coupling to the electric field gradient Q', and higher-order multipole interactions between $\vec{S}$ and $\vec{I}$. The spin Hamiltonian is written out in full in the papers already referred to. The parameters in it were determined by diagonalizing the spin Hamiltonian and fitting the results to the experimentally observed transition frequencies. Part of the results is displayed in Table I.

TABLE I. SPIN HAMILTONIAN PARAMETERS FOR Mn^{2+}, EXPRESSED IN MHz, AS DERIVED FROM ENDOR AT 4.2 K

	K_2MgF_4	K_2ZnF_4	K_2CdF_4	Rb_2MgF_4	Rb_2ZnF_4	Rb_2CdF_4
A/h	-272.24	-269.633	-268.994	-271.674	-268.738	-269.528
B/h	-271.84	-270.606	-271.643	-272.994	-270.987	-271.529
Q'/h	+0.19	-0.564	-1.215	-0.705	-1.144	-0.931

It may be stated merely that the nuclear quadrupole coupling can be understood quite accurately on the basis of a point charge model calculation [70]. Another aspect of the axial symmetry in these compounds is the anisotropy of the hyperfine structure. No anisotropy in the hyperfine interaction would be expected if the ground state of the Mn^{2+} were a pure S-state. However, perturbations due to the axial crystalline field potential W_{ax} will admix excited configurations such as $3d^44s$ into the ground state with coefficients like $\langle 3d^44s\ {}^6D | W_{ax} | 3d^5\ {}^6S \rangle / \{E(3d^44s\ {}^6D) - E(3d^5\ {}^6S)\}$. Such admixtures will give rise to an anisotropic part in the hyperfine interaction, for instance through electron-nuclear dipole-dipole interaction. On the basis of this mechanism one expects a contribution to the hyperfine anisotropy that is proportional to W_{ax}. Since, on the other hand, the nuclear quadrupole coupling will also be proportional to W_{ax} at the nuclear site, this treatment predicts a linear relationship between the hyperfine anisotropy and the nuclear quadrupole coupling. That such a dependence really exists is borne out by the experimental results as shown in Fig. 11. Six of the data points in Fig. 11 are taken from Table I, the others are from various sources in the literature [69, 71-78]. It is seen that the experimental evidence supporting a linear relationship is quite substantial. Here ENDOR sets a beautiful example of its potentialities: the small value of the anisotropy, between 0.1 and 1%, can easily be measured with great accuracy.

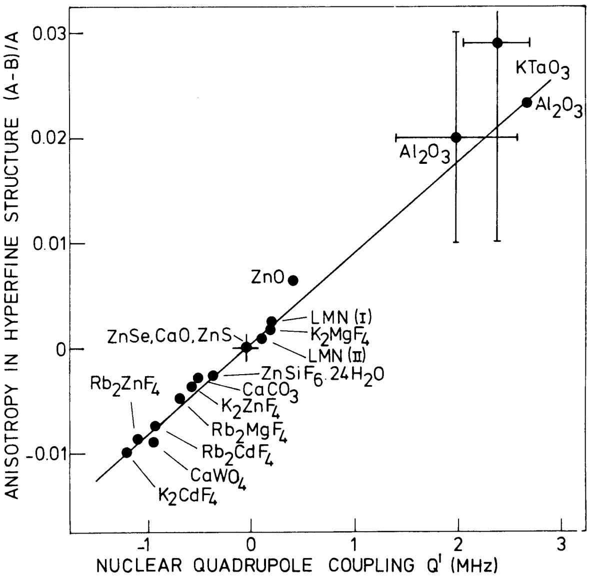

FIG. 11. Relative anisotropy in the hyperfine structure of Mn^{2+} in various compounds plotted against nuclear quadrupole coupling constant.

Another topic Schrama deals with in his papers is the important concept of zero-point spin reduction in the antiferromagnetic compounds K_2MnF_4 and Rb_2MnF_4. Paying due attention to differences in lattice parameters and degree of covalency he is able to deduce a value for A_{af} in the manganese compounds starting from his measured values in the manganese-doped Mg, Zn, and Cd compounds. This value is: $A_{af}/hc = -91.9 \times 10^{-4}\ cm^{-1}$. From NMR in the ordered state the hyperfine fields $A_{af}\langle S_z \rangle$ at the nuclear sites are known: $A_{af}\langle S_z \rangle /h = 643.5$ MHz for K_2MnF_4 and 642.4 MHz for Rb_2MnF_4 [79]. Comparing these data one obtains for the expectation value of the spin $\langle S_z \rangle = 2.33$, representing a spin deviation of 0.17 with respect to $S = 5/2$. Such a reduction was actually predicted on the basis of spin-wave theory [80] for two-dimensional lattices with antiferromagnetic coupling between the spins. The compounds studied are actually examples of quadratic layer antiferromagnets. A smaller value for the spin reduction, $\Delta S = -0.08$, is given by spin-wave theory for three-dimensional magnetic lattices. Fitting nicely within this framework are the results for $KMnF_3$ and $RbMnF_3$. These compounds, which crystallize in the cubic perovskite structure, show antiferromagnetic interactions in three dimensions. To obtain the value of A_{af} ENDOR measurements were again performed in a series of manganese-doped isomorphous compounds, this time consisting of $KMgF_3$, $KZnF_3$, $KCdF_3$, and $RbCdF_3$ [68,81]. To bring theory and experiment into agreement it proved necessary to include an arbitrary enhancement factor of 2.3 into the calculation of the supertransferred hyperfine interaction [82-85]. This concerns the interaction between a manganese nuclear spin and the electron spin of nearest neighbour manganese ions. Certainly this discrepancy has still to be clarified.

6. SILICON

6.1. Shallow donors

As the first demonstration of the ENDOR method was carried out successfully on the system P in Si [3], it is not surprising that soon afterwards a much more detailed study of the shallow donors P, As and Sb in silicon appeared [5]. Repeating these investigations more than ten years later with the stationary ENDOR method, Hale and Mieher [13] were able to achieve a considerable improvement. Not only their accuracy was better but also the hyperfine interaction with many more ^{29}Si nuclei could be resolved. ^{29}Si is the 4.7% abundant only stable isotope of silicon with $I \neq 0$. To take the hyperfine interaction between a donor electron and a nucleus into account properly an interaction tensor $\overleftrightarrow{A}$ has to be used. This tensor is conveniently separated into an isotropic part $a\overleftrightarrow{1}$ and an anisotropic traceless tensor $\overleftrightarrow{B}$: $\overleftrightarrow{A} = a\overleftrightarrow{1} + \overleftrightarrow{B}$. The isotropic interaction originates from the finite probability of finding the electron inside a nucleus. For this so-called contact interaction Fermi [86] derived the expression:

$$a_j = (8\pi/3) g_e g_N \mu_B \mu_N |\phi(\vec{r}_j)|^2$$

which relates the electron probability density at the nuclear site $\vec{r}_j$ to the measurable spin-Hamiltonian parameter a_j. The anisotropic part $\overleftrightarrow{B}$ is due to electron-nuclear dipole-dipole interactions which have the form

$$\mathcal{H}_{hf} = (\vec{\mu}_e \cdot \vec{\mu}_N)/r^3 - 3(\vec{\mu}_e \cdot \vec{r})\,(\vec{\mu}_N \cdot \vec{r})/r^5$$

To treat these hyperfine interactions the nuclei of the silicon lattice are grouped together into shells [13, 87]. Atoms that can be transformed into each other by a symmetry transformation of the point group of the silicon crystal, $\bar{4}3m$, belong to one and the same shell. It appears that there are four classes of shells with distinct symmetry properties. These classes are the {110}-plane, the $\langle 111 \rangle$-axis, and $\langle 001 \rangle$-axis classes for atoms lying on {110}-planes, $\langle 111 \rangle$-axes, and $\langle 001 \rangle$-axes, respectively. Lastly, there is the low symmetry class for atoms not belonging to any of the categories mentioned. An analysis of the angular dependence of the hyperfine interactions reveals characteristic differences between these four classes. Figure 12 is an illustration of this. For example, all the nuclei making up a shell of the {110}-plane class yield a pattern with 2 lines for $\vec{H}$ parallel to the [001]-direction, 3 for the [111]-direction, and 4 for the [110]-direction. These numbers, which form a combination unique for each class, allow one to determine the class to which the nucleus under study belongs.

For a further exact nuclear site location one has to rely upon more detailed theory. In the case of shallow donors this is the effective mass theory of Kohn and Luttinger [88]. In a series of papers successive refinements of the theory and the calculations were described, resulting finally in the assignment of more than 20 shells to specific lattice sites [89-95]. Thus, a detailed mapping of the electron wave function is obtained. Owing to interference effects in the effective mass wave functions, $|\phi(\vec{r})|^2$ does not decrease monotonically away from the donor atom. For instance, at the (0, 0, 1)-site the electron probability density is about ten times larger

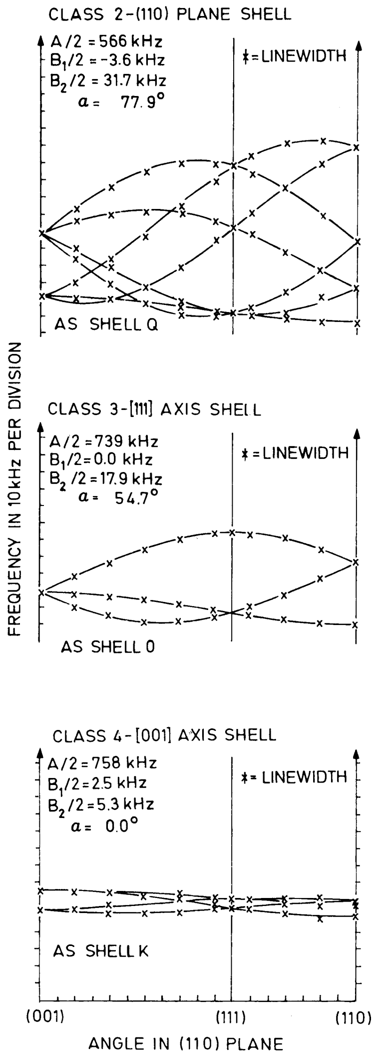

FIG. 12. Typical pattern for the angular dependence of ENDOR frequencies for the higher symmetry classes. Experimental data are from arsenic in silicon [13].

than at the nearest-neighbour site (1/4, 1/4, 1/4). The interference effects are related to $\vec{k}_0$, the positions of the minima of the conduction band in reciprocal space. A best match between theory and experiment requires $|\vec{k}_0| = 0.87k_{max}$.

Another shallow donor which was investigated by ENDOR is lithium [96] Lithium enters the silicon crystal as an interstitial impurity; its ionization energy is very well predicted by the effective mass theory. Nevertheless, the phenomena here are completely different from those in P, As and Sb.

This is due to the inverted level scheme of the lithium donor, in which the E and T_2-states lie lowest and the ground state therefore is orbitally degenerate. Saturation of the EPR transitions and ENDOR experiments are only possible after lifting this degeneracy by applying external stress. From the self ENDOR results it appears that the donor wave function depends strongly on temperature in the region from 1.3 to 4.2 K. For details of this profound study the original paper should be consulted.

No papers reporting ENDOR research on the shallow acceptors (B, Al, Ga, In) have been published so far.

6.2. Deep level impurities

When introduced into silicon many elements give rise to donor or acceptor levels deep in the gap between valence and conduction band. Among these impurities the transition metals vanadium, chromium, manganese and iron were studied by ENDOR [18]. It was found that the hyperfine interactions with the impurity nuclei are isotropic. This indicates that these impurities either occupy the substitutional sites in the silicon lattice, or the tetrahedral interstitial sites. In the absence of knowledge about ^{29}Si interactions it was not possible to discriminate between these two possibilities. For the deep donor sulphur ^{29}Si ENDOR was observed for eight shells of ^{29}Si nuclei around the donor site [87]. Attempts to understand the data on the basis of the effective mass theory were not successful. Since the ionization energy of the S^+ donor is 0.52 eV, a breakdown of the shallow donor theory had to be expected.

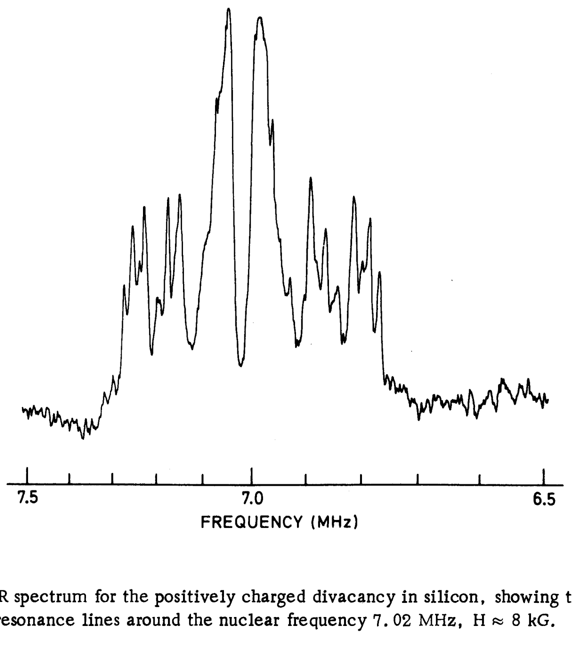

FIG. 13. ENDOR spectrum for the positively charged divacancy in silicon, showing the symmetrical arrangement of resonance lines around the nuclear frequency 7.02 MHz, H ≈ 8 kG.

From the expression in section 2.6 it follows that ENDOR transitions occur at frequencies symmetrically shifted up and down with respect to the nuclear frequency $g_N \mu_N H/h$. Such a symmetric pattern, taken from recent measurements in our laboratory on the divacancy in silicon [97], is shown in Fig.13. Obviously nuclear g-factors g_N can be calculated from the frequency ν_N at the centre of the pattern of resonance lines. Using this principle nuclear magnetic moments were measured by ENDOR for ^{32}P [4], ^{57}Fe [98] and ^{197}Au [99] after deliberately introducing these elements as impurities into silicon. In other occasions the situation is reversed: the identity of the impurity present in the sample being measured is unknown. From ENDOR it is then possible not only to determine the nuclear magnetic moment, but also, from the number of resonance lines, the nuclear angular momentum in units of $\hbar$. The identity of the impurity involved may then be looked up in a table of nuclear angular and magnetic momenta. Here ENDOR is used as an analytical tool. In this way the structure of four radiation damage centres in silicon, namely the phosphorus-vacancy [17], the aluminium-vacancy [100], and the arsenic- and antimony-vacancy pairs [101], was verified. In these cases ENDOR also yielded information on the distribution of the electron around the defect site. A powerful theory describing the electronic structure of the deep level defects is still lacking. Therefore an interpretation, reminiscent of the successes of the effective mass theory for the shallow level defects, remains to be developed in the future.

REFERENCES

[1] FEHER, G., Phys. Rev. 103 (1956) 500-1.
[2] FEHER, G., GERE, E.A., Phys. Rev. 103 (1956) 501-3.
[3] FEHER, G., Phys. Rev. 103 (1956) 834-35.
[4] FEHER, G., FULLER, C.S., GERE, E.A., Phys. Rev. 107 (1957) 1462-64.
[5] FEHER, G., Phys. Rev. 114 (1959) 1219-44.
[6] FEHER, G., Phys. Rev. 105 (1957) 1122-23.
[7] PORTIS, A.M., Phys. Rev. 91 (1953) 1071-78.
[8] HYDE, J.S., Phys. Rev. 119 (1960) 1492-95.
[9] KHUTSISHVILI, G.R., Zh. Ehksp. Teor. Fiz. 50 (1966) 1641-48; Sov. Phys.—JETP 23 (1966) 1092-96.
[10] ZHIDKOV, O.P., Fiz. Tverd. Tela 9 (1967) 3229-33; Sov. Phys.—Solid State 9 (1968) 2543-46.
[11] FEHER, G., Physica 24 Suppl. (1958) S80-87.
[12] SEIDEL, H., Z. Phys. 165 (1961) 239-52.
[13] HALE, E.B., MIEHER, R.L., Phys. Rev. 184 (1969) 739-50.
[14] LAMBE, J., LAURANCE, N., McIRVINE, E.C., TERHUNE, R.W., Phys. Rev. 122 (1961) 1161-70.
[15] SCHRAMA, A.H.M., J. Magn. Res. 6 (1972) 432-37.
[16] SEIDEL, H., Z. Phys. 165 (1961) 218-38.
[17] WATKINS, G.D., CORBETT, J.W., Phys. Rev. 134 (1964) A1359-77.
[18] WOODBURY, H.H., LUDWIG, G.W., Phys. Rev. 117 (1960) 102-8.
[19] ALGER, R.S., Electron Paramagnetic Resonance, Interscience Publishers, New York (1968).
[20] HARDEMAN, G.E.G., Philips Res. Reps. 15 (1960) 587-97.
[21] LEIFSON, O.S., JEFFRIES, C.D., Phys. Rev. 122 (1961) 1781-95.
[22] HOLTON, W.C., BLUM, H., Phys. Rev. 125 (1962) 89-103.
[23] CASTNER, T.G., DOYLE, A.M., Rev. Sci. Instrum. 39 (1968) 1090-91.
[24] DOYLE, W.T., DUTTON, T.F., LIU, H.P., Rev. Sci. Instrum. 40 (1969) 171-72.
[25] YAGI, H., INOUE, M., TATSUKAWA, T., YAMAMOTO, T., Jap. J. Appl. Phys. 9 (1970) 1386-90.
[26] YAGI, H., INOUE, M., TATSUKAWA, T., YAEGUCHI, O., KATO, S., Jap. J. Appl. Phys. 9 (1970) 1534.
[27] SCHMALBEIN, D., WITTE, A., RÖDER, R., LAUKIEN, G., Rev. Sci. Instrum. 43 (1972) 1664-67.
[28] DOYLE, W.T., DUTTON, T.F., WOLBARST, A.B., Rev. Sci. Instrum. 43 (1972) 1668-70.
[29] SEIDEL, H., WOLF, H.C., Phys. Stat. Sol. 11 (1965) 3-66.

[30] MARKHAM, J.J., Solid State Physics, Suppl. 8, Academic Press, New York (1966).
[31] FOWLER, W.B., Physics of Color Centers, Academic Press, New York (1968).
[32] HAUSMANN, A., SANDER, W., The Electronic Structure of Point Defects, North-Holland Publishing Company, Amsterdam (1971).
[33] DE WIJN, H.W., SCHRAMA, A.H.M., J. Chem. Phys. 49 (1968) 2971-73.
[34] MANOOGIAN, A., FRY, D.J.I., Proc. Conf. Magnetic Resonance and Relaxation, Ljubljana, 1966, North-Holland Publishing Company, Amsterdam (1967) 146-58.
[35] WOONTON, G.A., DYER, G.L., Can. J. Phys. 45 (1967) 2265-79.
[36] FREUND, P., OWEN, J., HANN, B.F., J. Phys. C 6 (1973) L139-43.
[37] ESKES, Y.H., DE WIJN, H.W., Phys. Lett. 25A (1967) 553-54.
[38] DYER, G.L., WOONTON, G.A., Can. J. Phys. 45 (1967) 2975-82.
[39] SROUBEK, Z., ŠIMÁNEK, E., ORBACH, R., Phys. Rev. Lett. 20 (1968) 391-92.
[40] SAXENA, G.P., VINCENT, C., Can. J. Phys. 49 (1971) 2276-81.
[41] FREUND, P., HANN, B.F., OWEN, J., J. Phys. C 4 (1971) L296-99.
[42] LOCHER, P.R., GESCHWIND, S., Phys. Rev. 139 (1965) A991-94.
[43] FRY, D.J.I., LLEWELLYN, P.M., Proc. Roy. Soc. A266 (1962) 84-92.
[44] HARDEMAN, G.E.G., Proc. 12th Coll. Ampère, Bordeaux, 1963, North-Holland Publishing Company, Amsterdam (1964) 334.
[45] HARDEMAN, G.E.G., J. Phys. Chem. Solids 24 (1963) 1223-31.
[46] MORIGAKI, K., HOSHINA, T., J. Phys. Soc. Japan 24 (1968) 120-26.
[47] VAN ENGELEN, P., VAN STAPELE, R.P., Fourth Symp. Magnetic Resonance, Rehovot and Jerusalem (1971).
[48] VAN ENGELEN, P., BOON, W., DIELEMAN, J., J. Phys. Chem. Solids 33 (1972) 1041-50.
[49] LUDWIG, G.W., LORENZ, M.R., Phys. Rev. 131 (1963) 601-4.
[50] CHEN, I., KIKUCHI, C., WATANABE, H., J. Chem. Phys. 42 (1965) 189-95.
[51] KRAVITZ, L.C., PIPER, W.W., Phys. Rev. 146 (1966) 322-29.
[52] CEDERQUIST, A., thesis, Washington University, St. Louis, 1963.
[53] HYDE, J.S., MAKI, A.H., J. Chem. Phys. 40 (1964) 3117-18.
[54] HYDE, J.S., J. Chem. Phys. 43 (1965) 1806-18.
[55] YAMAMOTO, T., SATO, K., MIYAMAE, T., Jap. J. Appl. Phys. 11 (1972) 1508-13.
[56] ATHERTON, N.M., BLACKHURST, A.J., COOK, I.P., Trans. Faraday Soc. 67 (1971) 2510-15.
[57] DINSE, K.P., BIEHL, R., MÖBIUS, K., HAUSTEIN, H., Chem. Phys. Lett. 12 (1971) 399-402.
[58] DINSE, K.P., BIEHL, R., MÖBIUS, K., PLATO, M., J. Magn. Res. 6 (1972) 444-52.
[59] ALLENDOERFER, R.D., MAKI, A.H., J. Magn. Res. 3 (1970) 396-410.
[60] LENIART, D.S., VEDRINE, J.C., HYDE, J.S., Chem. Phys. Lett. 6 (1970) 637-40.
[61] DINSE, K.P., MOBIUS, K., PLATO, M., BIEHL, R., HAUSTEIN, H., Chem. Phys. Lett. 14 (1972) 196-200.
[62] ALLENDOERFER, R.D., Chem. Phys. Lett. 17 (1972) 172-74.
[63] DOVGOPOL, S.P., IZYUMOVA, T.G., Zh. Ehksp. Teor. Fiz. 49 (1965) 1483-91; Sov. Phys. — JETP 22 (1966) 1018-23.
[64] GOKHMAN, V.L., ZEVIN, V.Ya., SHANINA, B.D., Fiz. Tverd. Tela 10 (1968) 337-50; Soviet Phys. — Solid State 10 (1968) 269-78.
[65] ZEVIN, V.Ya., BRIK, A.B., Ukr. Fiz. Zh. 17 (1972) 1688-98.
[66] FEHER, G., GERE, E.A., Phys. Rev. 114 (1959) 1245-56.
[67] WENCKEBACH, W.Th., POULIS, N.J., Proc. 17th Congr. Ampère, Turku, 1972, North-Holland Publishing Company, Amsterdam (1973) 120-42.
[68] SCHRAMA, A.H.M., WOUTERS, P.I.J., DE WIJN, H.W., Phys. Rev. B2 (1970) 1235-39.
[69] SCHRAMA, A.H.M., Proc. 16th Congr. Ampère, Bucharest (1970) 1103-8.
[70] SCHRAMA, A.H.M., Physica 68 (1973) 279-302.
[71] FOLEN, V.J., Phys. Rev. 125 (1962) 1581-83.
[72] CAVENETT, B.C., Proc. Phys. Soc. 84 (1964) 1-9.
[73] KREBS, J.J., LAMBE, J., LAURANCE, N., Phys. Rev. 141 (1966) 425-27.
[74] MIMS, W.B., DEVLIN, G.E., GESCHWIND, S., JACCARINO, V., Phys. Lett. 24A (1967) 481-82.
[75] HAUSMANN, A., HUPPERTZ, H., J. Phys. Chem. Solids 29 (1968) 1369-75.
[76] DE BEER, R., VAN ORMONDT, D., Phys. Lett. 27A (1968) 475-76.
[77] MANKOWITZ, J., LOW, W., Phys. Rev. B2 (1970) 28-32.
[78] HANNON, D.M., Phys. Rev. B3 (1971) 2153-58.
[79] WALSTEDT, R.E., DE WIJN, H.W., GUGGENHEIM, H.J., Phys. Rev. Lett. 25 (1970) 1119-22.
[80] ANDERSON, P.W., Phys. Rev. 86 (1952) 694-701.

[81] SCHRAMA, A.H.M., Physica 66 (1973) 131-44.
[82] OWEN, J., TAYLOR, D.R., Phys. Rev. Lett. 16 (1966) 1164-66.
[83] HUANG, N.L., ORBACH, R., ŠIMÁNEK, E., Phys. Rev. Lett. 17 (1966) 134-36.
[84] HUANG, N.L., ORBACH, R., ŠIMÁNEK, E., OWEN, J., TAYLOR, D.R., Phys. Rev. 156 (1967) 383-90.
[85] OWEN, J., TAYLOR, D.R., J. Appl. Phys. 39 (1968) 791-96.
[86] FERMI, E., Z. Phys. 60 (1930) 320-33.
[87] LUDWIG, G.W., Phys. Rev. 137 (1965) A1520-30.
[88] KOHN, W., Solid State Phys. 5 (1957) 257-320.
[89] HALE, E.B., MIEHER, R.L., Phys. Rev. 184 (1969) 751-59.
[90] HALE, E.B., MIEHER, R.L., Phys. Lett. 29A (1969) 350-51.
[91] HALE, E.B., CASTNER, T.G., Phys. Rev. B1 (1970) 4763-83.
[92] CASTNER, T.G., HALE, E.B., CRAVEN, R., Proc. 10th Conf. Physics of Semiconductors, Cambridge, Mass., (1970) 613-19.
[93] CASTNER, T.G., Phys. Rev. B2 (1970) 4911-42.
[94] HALE, E.B., MIEHER, R.L., Phys. Rev. B3 (1971) 1955-65.
[95] IVEY, J.L., MIEHER, R.L., Phys. Rev. Lett. 29 (1972) 176-78.
[96] WATKINS, G.D., HAM, F.S., Phys. Rev. B1 (1970) 4071-98.
[97] DE WIT, J.G., AMMERLAAN, C.A.J., SIEVERTS, E.G., Proc. Conf. Lattice Defects in Semiconductors, Freiburg, 1974.
[98] LUDWIG, G.W., WOODBURY, H.H., Phys. Rev. 117 (1960) 1286-87.
[99] WOODBURY, H.H., LUDWIG, G.W., Phys. Rev. 117 (1960) 1287-88.
[100] WATKINS, G.D., Phys. Rev. 155 (1967) 802-15.
[101] ELKIN, E.L., WATKINS, G.D., Phys. Rev. 174 (1968) 881-97.